Comparison of the influence of Ni and Zn impurities on the electromagnetic properties of $YBa_2Cu_3O_{6.95}$

D. A. Bonn, S. Kamal, Kuan Zhang, Ruixing Liang, D. J. Baar, E. Klein,* and W. N. Hardy
Department of Physics, University of British Columbia, Vancouver, British Columbia, Canada V6T 1Z1
(Received 29 November 1993)

A set of highly sensitive cavity perturbation techniques, quite different from the ones most commonly used to measure thin films, has been developed for measuring the surface impedance of small crystals of high-T_c superconductors. Since the results of these studies differ markedly from most surface-impedance measurements of thin films of high-T_c superconductors, we describe the techniques in detail, including recent improvements. Measurements of the surface resistance and penetration depth of a twin-free crystal of $YBa_2Cu_3O_{6.95}$ indicate two striking differences from the surface impedance of conventional superconductors. Both quantities exhibit linear temperature dependence at low temperatures rather than the exponentially activated behavior of an *s*-wave BCS superconductor. Also, a broad peak in the temperature dependence of the surface resistance indicates that the large transport scattering rate in the normal state collapses below T_c as the holes condense into the superconducting condensate. Systematic studies of the influence of Zn and Ni impurities on the surface impedance indicate that these properties are very sensitive to defects and this sensitivity provides further insight into the pairing state. Although both types of impurities provide strong elastic scattering that limits the collapse of the scattering rate and suppresses the peak in the surface resistance, only Zn has a strong pair-breaking effect. As little as 0.31% Zn substitution makes $YBa_2Cu_3O_{6.95}$ gapless, but Ni, which is a magnetic impurity has no such pair-breaking effect up to 0.75% substitution. This difference is the opposite of that expected for an *s*-wave BCS superconductor.

I. INTRODUCTION

One of the focal points of research on high-T_c superconductors, the nature of the pairing state, can be investigated by experimental techniques that are sensitive to the spectrum of low-lying excitations in the superconducting state. However, the small coherence length of $YBa_2Cu_3O_{7-\delta}$ gives rise to substantial complications for the experimental techniques traditionally used to probe the superconducting pairing state. Tunneling and far-infrared absorption, the two techniques that usually give the most direct and detailed information on a superconductor's energy gap and spectrum of low-lying excitations, are still subjects of controversy when applied to this high-T_c compound. Tunneling measurements are difficult in a material with a coherence length that is comparable to the lattice spacing, and measurements of the energy gap by various tunneling techniques remain controversial, particularly in $YBa_2Cu_3O_{7-\delta}$ where the results depend a great deal on the type of tunneling technique used.[1] The short coherence length also guarantees that pure $YBa_2Cu_3O_{7-\delta}$ is in the clean limit, which makes it difficult to measure an energy gap by far-infrared techniques.[2] Infrared measurements are further complicated by the presence of the midinfrared-absorption band and phonon anomalies that are the dominant features of the low-frequency optical conductivity.[3]

The high critical temperature complicates many other measurements that, in principle, can be used to help identify the superconducting pairing state. The temperature dependence of thermal conductivity, ultrasonic attenuation, and heat capacity can provide information on the thermally excited quasiparticles in the superconducting state. For instance, the presence of an *s*-wave BCS energy gap manifests itself as an exponentially activated temperature dependence in all of these quantities at temperatures well below T_c. Observation of power laws at low temperature would instead suggest a pairing state with nodes in the gap or gapless superconductivity. In $YBa_2Cu_3O_{7-\delta}$, however, in the temperature range of interest for probing the electronic excitations, these properties are all strongly influenced by phonon contributions.[4]

All of these difficulties make measurements of the low-frequency electromagnetic properties of $YBa_2Cu_3O_{7-\delta}$ particularly important. At microwave frequencies the surface impedance $Z_s = R_s + iX_S$, where R_s is the surface resistance and X_s is the surface reactance, is the measurable complex quantity that characterizes the electromagnetic properties of a superconductor. The surface reactance measures the screening of fields by the superconducting condensate and provides a direct measure of the London penetration depth via (in MKS units) $X_s(T) = \mu_0 \omega \lambda(T)$. The penetration depth can also be measured by magnetization and μSR techniques. The temperature dependence of $\lambda(T)$ determined from any of these techniques can provide information on the pairing state, but the measurements to date have been highly controversial. μSR is one of the few techniques that can measure the absolute value of $\lambda(0)$, but measurement of the temperature variation of λ has been complicated by sample dependences.[5-8] Another complication is that the muon relaxation rate is really a measure of field dis-

tribution in the vortex state, and some modeling of the vortex state is required in order to extract $\lambda(T)$. The degree to which this modeling affects the penetration depth extracted from μSR measurements is still an active area of study. Although the problems of sample dependence and modeling of the μSR lineshape are still being resolved, the most recent measurements, of crystals similar to the ones used for the measurements described in this paper, indicate a linear temperature dependence for the penetration depth below 30 K.[7]

Magnetization measurements of aligned powders of $YBa_2Cu_3O_{7-\delta}$ often indicate a nearly quadratic temperature dependence for $\lambda(T)$ in the *ab* plane.[9,10] Kinetic inductance measurements of the penetration depth in thin films of $YBa_2Cu_3O_{7-\delta}$ (Ref. 11) were also ultimately shown to be consistent with a quadratic temperature dependence in the penetration depth at low temperatures.[12] Early magnetization measurements of a single crystal of $YBa_2Cu_3O_{6.95}$ did not have sufficient precision to clearly discern the asymptotic behavior of $\lambda(T)$ at low temperature,[13] but a recent magnetization measurement of a $Tl_2Ba_2CaCu_2O_8$ crystal showed a dominant linear term.[14] A very large body of microwave measurements of $YBa_2Cu_3O_{7-\delta}$ has been plagued by sample dependence, and linear,[15] quadratic,[16–19] and exponentially activated[20] asymptotic behavior have all been reported, a nearly quadratic term being the most commonly observed in thin films. Recently, a distinctly linear term in $\lambda(T)$ has been observed in $YBa_2Cu_3O_{6.95}$ crystals, and it has been suggested that the T^2 term and sample dependence observed in thin films is the result of point defects or grain boundaries.[15] One possible explanation of a linear $\lambda(T)$ is a *d*-wave pairing state with line nodes in the gap function.[12] It is well known on theoretical grounds that strong potential scattering by defects can easily push such a superconductor into the gapless regime where a quadratic rather than linear term would be observed.[21,22] Therefore both the troublesome sample dependence in thin films and the possibility that $YBa_2Cu_3O_{7-\delta}$ might be a *d*-wave superconductor make it clear that studies of $\lambda(T)$ in carefully grown crystals with deliberately introduced defects are essential in this field.

The crucial role that defects play in the microwave properties of $YBa_2Cu_3O_{6.95}$ has already been demonstrated for the surface resistance.[23–26] Just as in the case of $\lambda(T)$, $R_s(T)$ in the crystals is qualitatively different from that observed in films. Whereas high purity crystals have a relatively high surface resistance with a broad peak near 40 K in the temperature dependence,[8,27,28] some high quality films exhibit a loss that is lower and that decreases monotonically with temperature. On the other hand, films also tend to suffer from substantial variation from sample to sample.[18,23,29] The high loss and nonmonotonic temperature dependence in single crystals have been attributed to a rapid decrease in the quasiparticle scattering rate below T_c.[8,27] In this scenario the presence of defects in the films are again the likely explanation for the difference between films and crystals. This view is strongly supported by systematic studies of $R_s(T)$ in Zn-doped crystals where it was found that the presence of Zn impurities limited the decrease in the scattering rate, suppressed the broad peak in $R_s(T)$, and lowered the overall loss, giving a surface resistance very similar to that observed in the lowest-loss thin films.[24,25]

The present paper brings together the results of a systematic study of the effects of Zn and Ni doping on the surface resistance and penetration depth of $YBa_2Cu_3O_{6.95}$ crystals. These two impurities are currently under close scrutiny because they both substitute for Cu in the CuO_2 planes, but have rather different effects on T_c and other physical properties. In Sec. II we will summarize the experimental techniques involved in our surface-impedance measurements, including recent refinements that have improved both the precision and absolute accuracy of the surface-resistance and penetration-depth measurements. Section III will focus on the surface impedance of undoped $YBa_2Cu_3O_{6.95}$ crystals, including recent measurements of the surface resistance of a twin-free crystal. The results of Zn and Ni doping will be presented in Sec. IV, and the interpretation of these results in terms of both a generalized two-fluid model and calculations for a *d*-wave pairing state will be discussed in Sec. V.

II. EXPERIMENTAL DETAILS

All of the measurements presented here have been obtained by cavity perturbation techniques using superconducting microwave resonators. When a small superconducting sample is inserted into a resonant cavity in a perturbation measurement, the small changes in the resonant frequency and Q of the cavity provide the means of measuring $X_s(T)$ and $R_s(T)$. The change in $1/Q$ of the cavity provides a relatively straightforward measure of the surface resistance via

$$\Delta\frac{1}{Q}=\left[\frac{1}{Q_s}-\frac{1}{Q_0}\right]\propto R_s\ , \tag{1}$$

where Q_0 is the Q of the empty cavity and Q_s is the Q of the cavity with the sample inserted. The relationship between the frequency shift and the surface reactance is complicated by the fact that the dominant effect of inserting a sample into a cavity is an overall shift of the resonant frequency by an amount proportional to V_s/V_r, where V_s is the sample volume and V_r is the effective volume of the resonator. The surface reactance is proportional to the penetration depth of the microwave fields and provides a relatively small frequency shift $\delta f\propto-\Delta V_s/V_r$, where ΔV_s is the volume of the sample penetrated by the microwave fields. δf is the frequency shift relative to that which would be measured for a sample with perfect screening and no penetration of the microwave fields. The net frequency shift is

$$\frac{\Delta f}{f_0}=\frac{f_s-f_0}{f_0}\propto\frac{V_s}{V_r}\left[1-\frac{\Delta V_s}{V_s}\right]\ , \tag{2}$$

where f_0 and f_s are the resonant frequencies of the unloaded and loaded cavity, respectively. In principle, both $R_s(T)$ and $X_s(T)$ can be measured in the same cavity, but the measurement of $X_s(T)$ is complicated by the large geometric frequency shift V_s/V_r. It is typically not possible to determine this shift, either by calculation or the

use of reference samples, with sufficient accuracy to obtain reliable absolute values of $X_s(T)$. Instead, the change in the reactance from its value at some base temperature T_0 is measured:

$$\Delta X_s(T)=\mu_0\omega\Delta\lambda(T)$$
$$=\mu_0\omega[\lambda(T)-\lambda(T_0)]$$
$$\propto -[f_s(T)-f_s(T_0)]\ . \quad (3)$$

Even with this compromise, it is difficult to measure $R_s(T)$ and $\Delta\lambda(T)$ in the same cavity with sufficient precision to yield useful information over the full range from low temperature to the normal state of a high-temperature superconductor. The central difficulty is that the measurements of very small R_s values in the superconducting state require careful measurement of Q_s and Q_0; thus, one must be able to move the sample in and out of the resonator to get a good measure of the small change in Q. Precise measurements of $\Delta X_s(T)$ have completely the opposite requirement. The sample must not be allowed to move during the course of the measurement or changes in the geometric shift, V_s/V_r, can contaminate or completely dominate $\Delta X_s(T)$. Our solution has been to design specialized resonators for these different measurements.

An early version of the resonator used to measure $\Delta X_s(T)$ has been described elsewhere.[15] The resonator is a split ring operating near 900 MHz and coated with a superconducting Pb:Sn alloy to give a Q of roughly 10^6. The requirements for measurements of $\Delta\lambda(T)$ to better than 1 Å are stringent: The resonator frequency must be stable to better than 1 Hz over the course of a measurement. The sample is mounted on a sapphire plate that holds the crystal in the homogeneous, axial, microwave magnetic field in the central bore of the split ring ($\mathbf{H}_{rf}\perp\hat{c}$). The rest of the sample holder is designed to minimize any motion of the sample as the temperature is changed: The sapphire plate is attached to a sapphire block where the sample heater and thermometer are located and the rest of the resonator assembly is at the temperature of the regulated 1.3-K He bath, and the temperature gradient between the sapphire block and the bath is sustained by a quartz tube. The rigidity and very low thermal expansion of the quartz tube minimize any sample motion over the relevant temperature range 1.3–100 K. A series of measurements with the sample at different positions (in the first version of the resonator) indicated that the magnetic field is homogeneous enough that motion of the sample in these fields is not a significant source of error. However, motion of the sapphire plate in the inhomogeneous electric fields is a more difficult problem. This source of systematic error has been further reduced in a new version of the resonator that has a rectangular rather than a square bore. The flatter shape allows the sample to be mounted farther away from the strong electric fields near the gap in the split ring and also improves the homogeneity of the electric fields in the region where the sample resides. The new apparatus is capable of resolving frequency shifts of a few tenths of a hertz, which, for a typical sample size, allows measurements of $\Delta\lambda(T)$ to a few tenths of 1 Å.

The calibration of the resonator was done with measurements on a Pb:Sn alloy sample with a T_c of 7.2 K. One can define a frequency shift δf and change in Q, $\delta(1/Q)$, for a loaded resonator relative to the frequency and Q of a sample that completely excludes the microwave fields. These quantities are actually measurable for the normal state of the Pb:Sn sample because the superconducting state is close to behaving like a perfect conductor with very low surface resistance and negligible penetration relative to the normal-state skin depth. Hence $\delta(1/Q(T))=1/Q(T)-1/Q(1.3\text{ K})$ and $\delta f=f(T)-f(1.3\text{ K})$. For Pb:Sn in the normal state, the classical skin effect should hold accurately at 900 MHz and both $\delta(1/Q)$ and $2\delta f/f$ should be proportional to the classical skin depth, which can be determined from the dc resistivity via $\delta_{cl}=(2\rho_{dc}/\mu_0\omega)^{1/2}$. Indeed, $\delta(1/Q)$ tracks the temperature dependence of δ_{cl} very well, but thermal expansion of the sample causes $2\delta f/f$ to deviate somewhat. Corrections for the thermal expansion brought both quantities into agreement with δ_{cl}, as shown in Fig. 1. For the purpose of calibrating the frequency-shift measurements, we actually made use of the relationship $\delta(1/Q)=2\delta f/f$ for a metallic slab in order to obtain δf from the measurements of $\delta(1/Q)$ of the Pb:Sn sample. For our measurement geometry, the frequency shift associated with a metallic sample in the classical skin-effect regime can be expressed as

$$\delta f=K_n A\delta_{cl}\ , \quad (4)$$

where A is the area of the slab-shaped sample. Thus, with measurements of $\delta(1/Q)$, the dc resistivity, and the area of the sample, one can use Eq. (4) to obtain the cali-

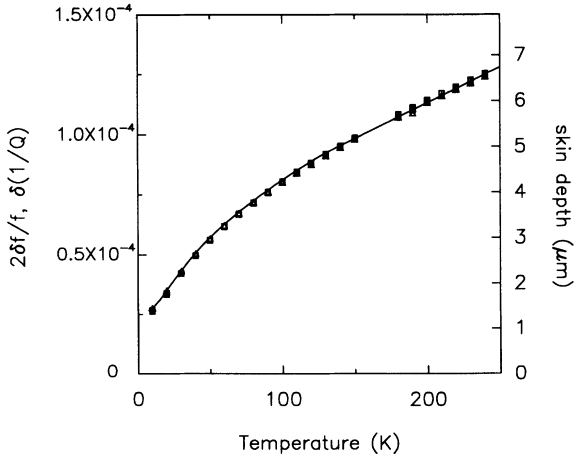

FIG. 1. Comparison of the classical skin depth (solid line) of a Pb:Sn reference sample and the $2\delta f/f$ (triangles) and $\delta(1/Q)$ (squares) measurements performed in the split-ring resonator used for the measurement of $\Delta\lambda(T)$. The skin depth is determined from dc resistivity measurements with the use of the classical skin-effect expression $\delta_{cl}=(2\rho_{dc}/\mu_0\omega)^{1/2}$. The agreement between all of these quantities indicates that the Pb:Sn alloy is in the classical skin-effect regime and this is used to find the calibration constant connecting δf and $\Delta\lambda$ in the superconducting state.

bration constant K_n. With this calibration the London penetration depth in the superconducting state can be obtained from

$$\Delta\lambda(T)=\frac{\delta f(T)}{2K_n A} . \quad (5)$$

The difference in the propagation constant in the normal and superconducting states is responsible for the factor of 2 difference in the calibration constants that appear in Eqs. (4) and (5). One small correction is made to the data before Eq. (5) is used to convert frequency shifts to penetration depths: There is a small temperature-dependent frequency shift for the bare sapphire sample holder that is subtracted from the data set. This amounts to roughly a 20% correction for measurements at 7 K where the shift associated with $\Delta\lambda$ is small, typically about 12 Hz, and paramagnetic impurities in the sapphire give a noticeable temperature dependence of -2 Hz to the frequency shift measured for a bare piece of sapphire. At higher temperatures the frequency shift due to the sample completely dominates any temperature dependence associated with the sapphire.

Surface-resistance measurements were made with two different resonators: a cylindrical cavity operated in the TE_{011} mode at 34.8 GHz and a split-ring resonator near 4 GHz.[30] Both resonators were coated with Pb:Sn, which gives a Q_0 of 2×10^6 for the split-ring resonator and 1×10^7 for the cylindrical cavity. In both systems the sample is mounted on a sapphire rod, which can be withdrawn for measurement of Q_0, and then reinserted into the axial magnetic fields of the cavity ($\mathbf{H}_{rf}\|\hat{c}$) such that currents are driven in the *ab* plane of the crystal. The calibration constant that connects the $\Delta(1/Q)$ measured in this way with R_s has been determined in two ways. At 34.8 GHz the skin depth in the normal state of $YBa_2Cu_3O_{6.95}$ is shallow enough that the classical skin-effect formula can be applied directly to the measured surface resistance. Thus a measurement of the dc resistivity which gives R_s in the normal state and a measurement of $\Delta(1/Q)$ at the same temperature in the normal state can be used to obtain an internal calibration for each crystal. On the other hand, near 4 GHz the skin depth is comparable to the thickness of some of the crystals and this gives an enhanced $\Delta(1/Q)$ in the normal state that precludes using the previously described procedure. Instead, calibration is done by measuring $\Delta(1/Q)$ in the normal state of a Pb:Sn sample cut to the same size as the crystal. Measurements of crystals that are thick enough to use both calibration techniques give absolute values that agree to $\pm5\%$.

The Pb:Sn samples are also used to correct for small nonperturbative effects in the resonators. The values of $\Delta(1/Q)$ for $YBa_2Cu_3O_{6.95}$ measured at low temperature are close to 10^{-7} in the cylindrical resonator and 10^{-8} in the split-ring resonator. At this level, nonperturbative contributions to $\Delta(1/Q)$ due to slight rearrangement of the microwave field pattern can be comparable to the contribution to $\Delta(1/Q)$ from actual loss in the sample. In order to measure the low-temperature residual loss of the samples, this extraneous contribution to $\Delta(1/Q)$ had to be measured and subtracted from the data. Measurement of the temperature dependence of $\Delta(1/Q)$ for several different samples of Pb:Sn all show the rapid drop in loss expected for a conventional superconductor at low temperatures and then run into a sample-independent $\Delta(1/Q)$ by 2 K. Since it is unlikely that residual loss in the Pb:Sn samples would be the same from sample to sample, we attribute this limiting $\Delta(1/Q)$ to nonperturbative effects and subtract it from the $YBa_2Cu_3O_{6.95}$ data sets. At 3.88 GHz this correction amounts to $\Delta(1/Q)\sim10^{-9}$ or a correction of roughly 7 $\mu\Omega$ in $R_s(T)$, about 10% of the loss of a typical $YBa_2Cu_3O_{6.95}$ crystal at 40 K. At 34.8 GHz the correction is typically less than 5% of the 40-K loss or about 100 $\mu\Omega$.

Finally, a dominant limitation on the sensitivity of our earlier loss measurements with these superconducting resonators was the presence of microphonics. When the Q is very high, even a very slight vibration of the sample in a resonator's fields leads to a modulation of the resonant frequency, which limits the accuracy of the measurement of $\Delta(1/Q)$. Particularly for the split-ring resonator, a reduction of the microphonics has led to a significant improvement in the precision of the measurements.

III. HIGH PURITY CRYSTALS

The measurements presented here of the surface impedance of crystals of $YBa_2Cu_3O_{6.95}$ are a continuation of studies already reported in the literature.[8,15,27] The crystals are grown by a flux-growth technique described in detail elsewhere.[31] Despite the fact that high purity starting materials are used, microwave measurements and elemental analysis by inductively coupled plasma (ICP) mass spectroscopy both indicate that the crystals typically contain $\sim0.1\%$ impurities. The most likely source of this contamination is impurities introduced into the melt as the flux corrodes the zirconia crucible. The crystals are very homogeneous, with T_c's near 93.4 K and a transition width of only 0.25 K as seen in the specific-heat jump, which provides a *bulk* measure of the transition.

A. Penetration depth

Figure 2 displays $\Delta\lambda(T)=\lambda(T)-\lambda(1.3\text{ K})$ for two typical crystals. As has been discussed previously, the measurement geometry used here, with $\mathbf{H}_{rf}\perp\hat{c}$, involves currents running in the $\hat{c}$ direction as well as the *ab* plane.[15] Provided that $\lambda_{ab}\ll c$ and $\lambda_c\ll a,b$, the measured $\Delta\lambda$ in this geometry is given by $\Delta\lambda=a\Delta\lambda_{ab}+c\Delta\lambda_c$, where a is the width of the crystal in the *ab* plane and c is the thickness. Since $\lambda_c/\lambda_{ab}\sim7$, the very thin samples ($a/c\sim20$) that we measure only involve contributions from λ_c at the 10–15% level. Both data sets shown in Fig. 2 have a nearly linear temperature dependence between 5 and 25 K that is in good agreement with our earlier measurements.[15] Recent measurements on a similar crystal at 17 GHz with $\mathbf{H}_{rf}\|\hat{c}$ are similar and have confirmed the linear temperature dependence in a geometry that measures only $\Delta\lambda_{ab}$.[32] The improved sensitivity of the measurements more clearly reveals a slight curvature below 5 K that we find to be

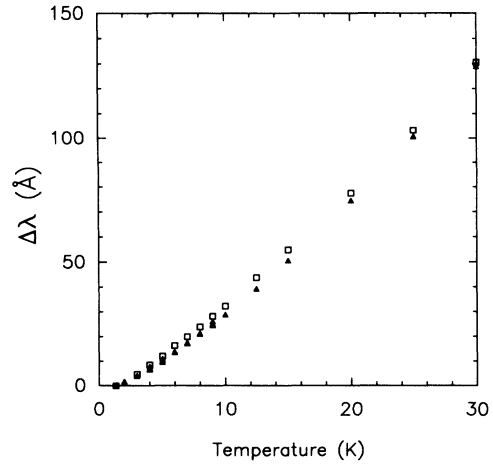

FIG. 2. The low-temperature behavior of $\Delta\lambda(T) = \lambda(T) - \lambda(1.3\text{ K})$ for two different crystals of $YBa_2Cu_3O_{6.95}$ is nearly linear between 5 and 25 K, with a small sample-dependent curvature at the lowest temperatures.

somewhat sample dependent. Variation from sample to sample might arise from variation in defect concentration from crystal to crystal or from different λ_c contributions due to different thicknesses.

Although $\Delta\lambda(T)$ is the quantity that is directly accessible by microwave measurements, it is useful to construct the quantity $x_s(T) = \lambda^2(0)/\lambda^2(T)$, which is a measure of the superfluid fraction. This quantity can be generated by adding 3 Å to the data shown in Fig. 2 in order to take into account the fact that the measurements are relative to the value at 1.3 K rather than $T = 0$ and then choosing a value of $\lambda(0)$. The resulting quantity shown in Fig. 3 has been generated with $\lambda(0) = 1400$ Å, close to the value suggested by far-infrared[33] and μSR (Ref. 8) measurements performed on similar crystals. The superfluid density has a nearly linear temperature dependence between 5 and 35 K with a slope, $dx_s/dt = -0.52$, where t is the reduced temperature, T/T_c. The slope at T_c is -3.0, 50% steeper than that of a weak-coupling BCS superconductor.

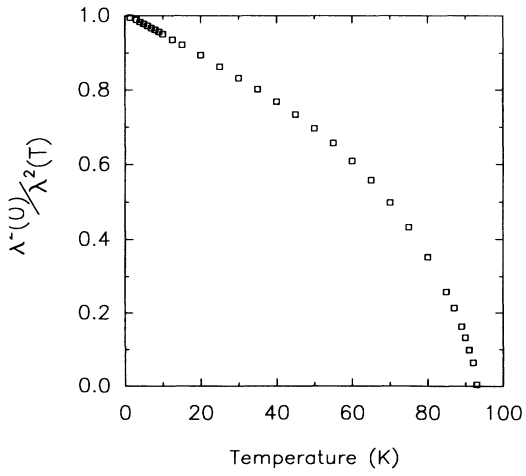

FIG. 3. The quantity $\lambda^2(0)/\lambda^2(T)$ gives the temperature dependence of the superfluid fraction $x_s(T)$. The linear asymptotic behavior below 35 K is clear as well as a steep slope in the regime near T_c. The values in this figure are derived from the data shown in Fig. 2 by assuming a value of 1400 Å for $\lambda(0)$.

B. Surface resistance

Figure 4 displays the surface resistance of a twin-free crystal measured at 4.13 and 34.8 GHz. The main qualitative features—the rapid drop at T_c, the broad peak near 40 K, and the rather weak temperature dependence below the peak—are all nearly the same as those observed in earlier measurements.[25,26] However, the improvements in measurement technique and the use of a twin-free sample have led to a few differences in detail. The minimum in $R_s(T)$ near 75 K is deeper in the twin-free crystal. We find that morphological defects such as growth steps and twin boundaries often cause some filling in of this minimum, particularly in the lower-frequency measurements. Also, the peak in $R_s(T)$ at 4.13 GHz is larger in amplitude and centered at a slightly lower temperature than it is in our previously published data.[26] Most importantly, the residual microwave loss at low temperatures is lower than that found in twinned crystals, less than 5 $\mu\Omega$ at 4.13 GHz and less than 150 $\mu\Omega$ at 34.8 GHz.

Although the surface impedance is the experimentally accessible quantity in microwave techniques, the complex conductivity $\sigma = \sigma_1 - i\sigma_2$ (for the convention $J \sim J_0 e^{i\omega t}$) makes closer contact with the microscopic properties of the material. In MKS units the surface impedance is given by

$$Z_s = R_s + iX_s = \left[\frac{i\mu_0\omega}{\sigma_1 - i\sigma_2}\right]^{1/2} \tag{6}$$

for the case of local electrodynamics. Fortunately, the short mean free path l in the normal state and the short

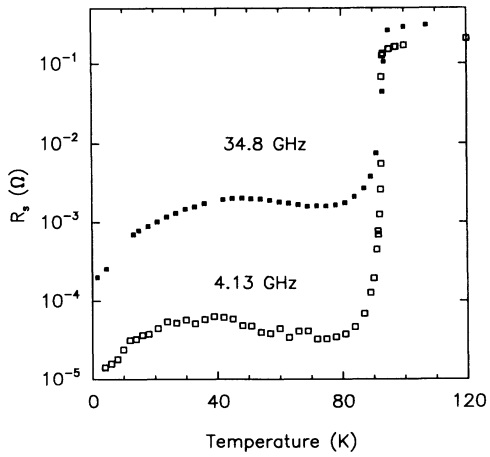

FIG. 4. *ab*-plane surface resistance of a twin-free crystal of $YBa_2Cu_3O_{6.95}$ measured at 4.13 and 34.8 GHz. The lack of twin boundaries has led to a lower residual loss than that typically observed in twinned crystals.

coherence length ξ_0 in the superconducting state guarantee that simple, local electrodynamics are adequate for calculating the properties $YBa_2Cu_3O_{6.95}$. Equation (6) can be used to derive a general expression for determining σ_1:

$$\sigma_1=\left\{\left[\frac{\sigma_s}{2}\pm\left[\frac{\sigma_s^2}{4}-\sigma_2\sigma_s\right]^{1/2}\right]^2-\sigma_2^2\right\}^{1/2}, \quad (7)$$

where the + (−) sign is used for the case $\sigma_1>$ ($<$) $\sqrt{3}\sigma_2$. σ_s is a measurable quantity

$$\sigma_s=\frac{\mu_0\omega}{2R_s^2}, \quad (8)$$

which can be determined from surface-resistance measurements, and corresponds to the value of σ_1 in the case of a normal metal (where $\sigma_1\gg\sigma_2$) in the classical skin-effect regime (local electrodynamics). Equation (7) is useful in the superconducting state because σ_2 depends only on the London penetration depth at low frequencies. In the superconducting state, the conductivity may be expressed as

$$\sigma(\omega,T)=\sigma^*(\omega,T)-i\frac{1}{\mu_0\omega\lambda^2(T)}, \quad (9)$$

where the second term is the screening response of the superfluid and the first term contains all other contributions to the conductivity. At low frequency ($\omega\tau\ll1$, where τ is the transport lifetime), σ^* has only a real part σ_1 and penetration depth measurements can then be used to determine the imaginary part via $\sigma_2=(\mu_0\omega\lambda^2)^{-1}$. Thus, in the superconducting state, we use Eq. (7) to extract σ_1 from measurements of R_s and λ. In the superconducting state, except for a small temperature range near T_c, $\sigma_1\ll\sigma_2$, and Eq. (7) reduces to

$$\sigma_1(\omega,T)=\frac{2R_s(\omega,T)}{\mu_0^2\omega^2\lambda^3(T)}. \quad (10)$$

Although we use Eq. (7) to analyze our data, Eq. (10) is much more transparent than Eq. (7) and is useful for understanding the factors that contribute to the measured surface resistance.

Figure 5 displays the real part of the conductivity extracted from the penetration depth shown in Fig. 3 and the surface resistances shown in Fig. 4. The large, broad peak in $\sigma_1(T)$ is the feature responsible for the nonmonotonic behavior of $R_s(T)$ in the single crystals, although the temperature dependence of the screening term $\omega^2\lambda^3(T)$ makes the feature less pronounced in $R_s(T)$. Similar peaks have been observed in THz spectroscopy on films that continue the trend observed in the crystals: The peak diminishes and shifts to higher temperature with increasing frequency.[34] The peak in $\sigma_1(T)$ is quite different from the coherence peak of an s-wave BCS superconductor which rises abruptly just below T_c and peaks at a higher temperature as well. Rather than being a coherence peak, broad peaks at low frequency in $\sigma_1(T)$ have been attributed to a rapid decrease below T_c in the quasiparticle scattering rate.[8,27,34,35] A very similar peak

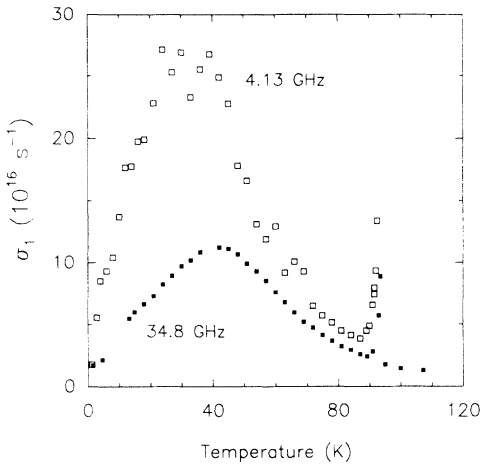

FIG. 5. *ab*-plane conductivity of the twin-free crystal of $YBa_2Cu_3O_{6.95}$ extracted from the $R_s(T)$ and $\lambda(T)$ measurements shown in Figs. 3 and 4. The broad peak in the conductivity results from competition between the decrease in the normal-fluid density below T_c and a quasiparticle lifetime that increases rapidly below T_c. Below 40 K the large difference between the conductivities at 4.13 and 34.8 GHz is additional confirmation that $\tau(T)$ increases 100-fold by 40 K, giving rise to relaxation effects when $\omega\tau(T)\sim1$ at 34.8 GHz.

in the thermal conductivity has been explained in the same way,[37] although the phonon contribution to the thermal conductivity complicates the interpretation of the thermal conductivity.[38,39] The behavior of the far-infrared optical conductivity of $Bi_2Sr_2CaCu_2O_8$ (Ref. 36) and $YBa_2Cu_3O_{6.95}$ (Ref. 33) has also been interpreted in terms of a rapid decrease in the scattering rate below T_c.

The broad peak in $\sigma_1(T)$ can be understood, at least qualitatively, in the context of a two-fluid model of the low-frequency conductivity. The real part of the conductivity can be divided into two terms[8,40]

$$\sigma_1(\omega,T)=\frac{ne^2}{m^*}\left[x_s(T)\delta(0)+x_n(T)\frac{\tau(T)}{1+\omega^2\tau^2(T)}\right]. \quad (11)$$

The first term is the superfluid response, which is responsible for the zero resistance at dc and also gives rise to the London screening term that dominates $\sigma_2(\omega,T)$. Measurements of the London penetration depth provide a measure of this superfluid fraction via $x_s(T)=\lambda^2(0)/\lambda^2(T)$. The second term in Eq. (11) is the normal-fluid response that is distributed over a range of frequencies and is modeled here with a simple Drude response. A sum rule governs the total area under $\sigma_1(\omega)$, and therefore the total oscillator strength is shared between the superfluid fraction $x_s(T)$ and the normal-fluid fraction $x_n(T)$. In the clean limit ($l\gg\xi_0$), all of the oscillator strength associated with the total free carrier density n is apportioned between these two terms so that $x_s(T)+x_n(T)=1$. This scenario is confirmed by far-infrared measurements which show that virtually all of the free-carrier conductivity seen in the normal state ultimately collapses into the superfluid screening term at low temperatures.[41] At intermediate temperatures, $x_n(T)$ decreases as T drops below T_c and $x_s(T)$ builds up. Thus a

broad peak in $\sigma_1(T)$ can result from competition between this decrease in $x_n(T)$ and a rapid increase in $\tau(T)$. Estimates based on Eq. (11) indicate that in $YBa_2Cu_3O_{6.95}$, $\tau(T)$ increases nearly two orders of magnitude before running into a limit due to impurities, at which point the temperature dependence of $x_n(T)$ wins out and causes the conductivity to decrease with decreasing temperature.

The huge increase in $\tau(T)$ implied by the 4.13-GHz measurements indicates that for the 34.8-GHz measurements $\omega\tau(T)$ should be of order unity below 30 K. This brings relaxation effects into play in the higher-frequency data where the denominator of the normal-fluid term in Eq. (11) tends to diminish the size of the peak in $\sigma_1(T)$ and shift it to higher temperature. This observed difference between the 4.13- and 34.8-GHz data is separate confirmation that the quasiparticle lifetime does increase dramatically below T_c. Above T_c, far-infrared measurements indicate that $\omega\tau(T)\sim 1$ at ~ 2400 GHz,[41] and so the observation of relaxation effects at 34.8 GHz is consistent with an increase in $\tau(T)$ by two orders of magnitude. This interpretation is also consistent with the smaller peak in $\sigma_1(T)$ observed at THz frequencies.[34]

Finally, the asymptotic behavior of $\sigma_1(T)$ at the two measurement frequencies should be noted. At 34.8 GHz, $\sigma_1(T)$ is quite linear below 30 K. Although somewhat noisier, the data at 4.13 GHz also vary linearly with temperature below 24 K. At both frequencies some sample-dependent curvature is often observed below 5 K, similar to the sample-dependent curvature observed in $\Delta\lambda(T)$ at low temperatures. The twin-free crystal has the most linear conductivity that we have observed, suggesting that any curvature in $\sigma_1(T)$ at low temperatures is probably due to defects, either impurities or twin boundaries. The asymptotic behavior of $\Delta\lambda(T)$ and $\sigma_1(T)$ will be discussed further in Sec. V, but it is at least worth noting here that none of these measurements have the exponentially activated behavior expected for an s-wave BCS superconductor.

IV. ZINC AND NICKEL IMPURITIES

As was discussed in the Introduction, the possibility that defects are responsible for much of the sample variation encountered in surface-impedance measurements of $YBa_2Cu_3O_{7-\delta}$ was a prime motivation for studying the effects that deliberately introduced impurities have on the surface impedance of single crystals. The observed properties of the high purity crystals suggest two types of effects. First, one can study the effect that impurities have on the quasiparticle lifetime. If there is indeed a 100-fold increase in $\tau(T)$ in the clean crystals, then the deliberate addition of impurities should place a limit on this increase, resulting in a decrease in the amplitude of the peak in $\sigma_1(T)$ and elimination of the relaxation effects at 34.8 GHz. Second, the possibility that $YBa_2Cu_3O_{6.95}$ might be made gapless by the addition of a modest level of impurities makes measurement of $\Delta\lambda(T)$ in impurity-doped crystals imperative.

Zn and Ni have been found to preferentially substitute for the Cu(2) atoms in the $YBa_2Cu_3O_{7-\delta}$ crystal structure.[42,43] Thus they provide a well-controlled means of specifically disturbing the CuO_2 planes that are the key element common to all of the highest-T_c superconductors. The rather different effects that Zn and Ni have on the most basic properties such as T_c and the dc resistivity suggest that these dopants provide an important testing ground for models of high-T_c superconductors. Zn has been found to have a more drastic effect on T_c than Ni. Susceptibility measurements of T_c for our two batches of $YBa_2(Cu_{1-x}Zn_x)_3O_{6.95}$ with $x=0.0015$ and 0.0031 indicate that the suppression of T_c with impurity content is $\partial T_c/\partial x \sim 1260$, which is in good agreement with the early study of doped crystals by Chien, Wang, and Ong.[44] A batch of crystals with a Ni content of 0.0075 gave $\partial T_c/\partial x \sim 390$, which is in good agreement with a recent study of Ni-doped thin films[45] and indicates that Zn depresses T_c roughly 3 times more rapidly than Ni does. On the other hand, Ni is found to increase the dc resistivity above T_c as much, or more, than Zn.[45] That is, Ni provides at least as much scattering of the holes as Zn does, but has a much less drastic effect on T_c.

Figure 6(a) shows the striking effect that Zn impurities have on the penetration depth. Addition of 0.31% Zn is sufficient to completely disrupt the linear temperature dependence, leaving a nearly quadratic $\Delta\lambda(T)$. The 0.15% impurity level exhibits intermediate behavior that has also been observed in the $\mathbf{H}_{rf}\|\hat{c}$ field configuration for a crystal from the same batch.[32] This result demonstrates the sensitivity of $\Delta\lambda(T)$ to impurities and strong-

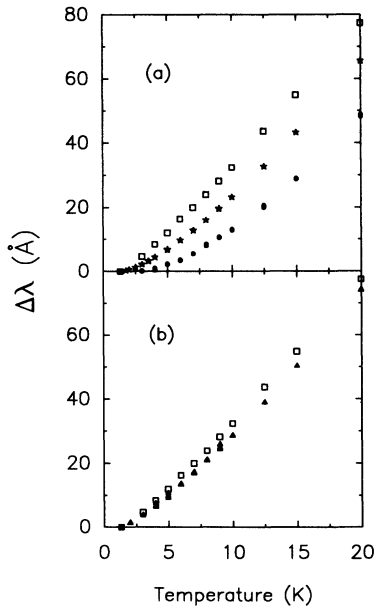

FIG. 6. Comparison of the effect of (a) Zn and (b) Ni impurities on the temperature dependence of the London penetration depth. The sequence shown in (a) from pure (squares) through 0.15% (stars) to 0.31% (solid circles) substitution of Zn for Cu shows a change from linear temperature dependence to the quadratic behavior expected for a gapless superconductor. On the other hand, (b) shows that 0.75% substitution of Ni impurities (solid triangles) has virtually no effect on the penetration depth.

ly suggest that defects are responsible for the sample-dependent quadratic behavior that is commonly observed in thin films of $YBa_2Cu_3O_{7-\delta}$. The effect of Ni impurities is in striking contrast to the Zn results. Figure 6(b) shows that a 0.75% Ni impurity level, more than twice the concentration of Zn required to completely alter the linear term, has almost no effect on $\Delta\lambda(T)$. To an even greater extent than the case of the suppression of T_c, the penetration-depth measurements show that Ni impurities disturb the superconducting pairing state of $YBa_2Cu_3O_{6.95}$ much less than Zn impurities do.

Our initial studies of the effect of Zn impurities on the surface resistance of $YBa_2Cu_3O_{6.95}$ have been presented elsewhere, and the only significant new feature of the results shown in Fig. 7 is that the residual loss at low temperature is somewhat lower. However, all of the results shown in Fig. 7 are for twinned crystals, including the high purity crystal. Twin-free Zn-doped crystals are not yet available, and so we can only draw conclusions from the effect that impurities have on the temperature dependence of the loss. As is the case with the measurements of $\Delta\lambda(T)$, the measurements of $R_s(T)$ demonstrate that the microwave properties of $YBa_2Cu_3O_{6.95}$ are extremely sensitive to impurities. The range of surface resistances shown in Fig. 7 covers much of the range of sample-dependent behavior observed in the best thin films, suggesting that the surface resistance of thin films is strongly influenced by defects of some sort. As shown in Fig. 8, Ni impurities are also very effective at suppressing the broad peak in $R_s(T)$, both at 3.88 and 34.8 GHz.

As was done for the twin-free crystal in Sec. III, the $R_s(T)$ and $\Delta\lambda(T)$ measurements can be used together to generate $\sigma_1(\omega,T)$ for the doped crystals. The only difficulty with this is that the dependence of $\lambda(0)$ on impurity content is not well known and a value of $\lambda(0)$ is needed to extract $\sigma_1(\omega,T)$ from the microwave measurements. However, at the rather low impurity concentrations studied here, it is reasonable to use the 1400-Å value assumed for the pure crystals. Since it is expected that impurities will increase $\lambda(0)$, this assumption leads to an overestimate of the magnitude of $\sigma_1(\omega,T)$ for the impurity-doped crystals, but does not affect the overall shape of the curves. Figure 9(a) and 9(b) show the conductivity of the Zn- and Ni-doped crystals, respectively, compared to a high purity crystal. Both impurities suppress the amplitude of the peak in $\sigma_1(T)$ and shift it to somewhat higher temperatures. The coherence peak of an s-wave BCS superconductor that has a large inelastic scattering rate should be little affected by the addition of the small level of impurities that we have used.[46,47] Thus the suppression of the peak in $\sigma_1(T)$ that we observe for low levels of impurities in $YBa_2Cu_3O_{6.95}$ is further evidence that the peak is not due to coherence effects. Instead, the observed suppression of the peak shows that the presence of impurities places a limit on the rapid increase in $\tau(T)$, which in turn limits the rise in $\sigma_1(T)$ below T_c. A further indication that these low levels of impurities are limiting the large increase in $\tau(T)$ is the disappearance of relaxation effects in the crystal with Ni impurities. In the context of a two-fluid model [see Eq. (11)], the large difference between the 3.88- and 34.8-GHz curves for the high purity crystal indicates that $\omega\tau\sim 1$ at 34.8 GHz and τ must have risen by two orders of magnitude below T_c. The addition of Ni then limits the increase in $\tau(T)$ enough that $\omega\tau \ll 1$ at 34.8 GHz and $\sigma_1(34.8\text{ GHz}, T)\sim\sigma_1(3.88\text{ GHz}, T)$.

A noteworthy difference between the effects of Zn and Ni impurities is apparent in Fig. 9. The low-temperature behavior of $\sigma_1(T)$ at 34.8 GHz for the Zn-doped series changes from the linear temperature dependence observed in the high purity crystal to a nearly quadratic temperature dependence of 0.31%, a progression that is similar to the effect of Zn on the low-temperature behavior of $\Delta\lambda(T)$. The Ni-doped sample shows no sign of this quadratic temperature dependence in either $\Delta\lambda(T)$

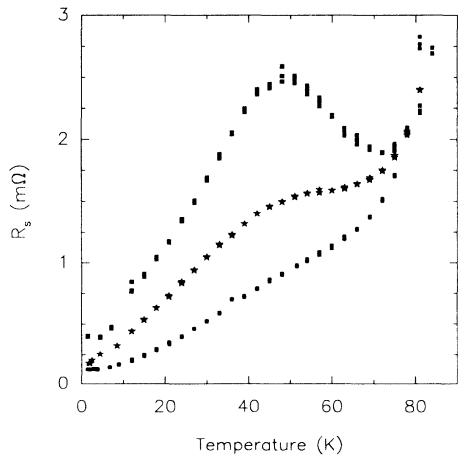

FIG. 7. Measurements of the surface resistance at 34.8 GHz demonstrate the strong influence that defects have on the microwave loss. The sequence from pure (solid squares) through 0.15% (stars) to 0.31% (solid circles) Zn substitution shows that the peak is suppressed and the overall loss is *decreased* by the addition of defects. The lowest curve is similar to that observed in the lowest-loss films.

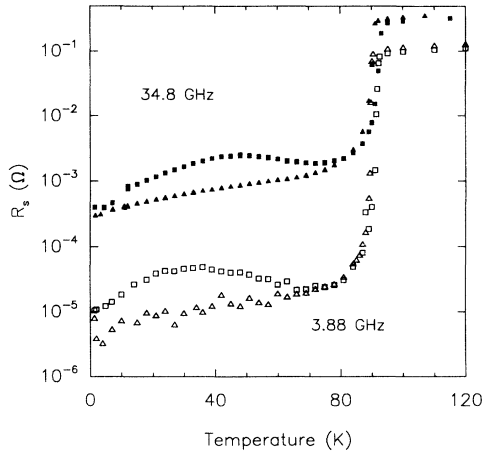

FIG. 8. Substitution of 0.75% Ni impurities (triangles) is sufficient to lower the overall loss and completely suppress the broad peak observed in the pure sample (squares) even though T_c is only decreased to 90.6 K.

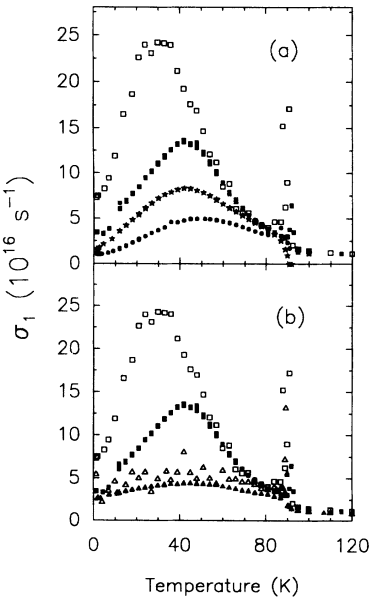

FIG. 9. Effect of (a) Zn and (b) Ni impurities on the conductivity. Both figures include the 3.88-GHz (open squares) and 34.8-GHz (solid squares) results for a high purity, twinned crystal. (a) shows that substitution with 0.15% (stars) and 0.31% (solid circles) Zn impurities suppresses the peak in the 34.8-GHz conductivity and shifts it to higher frequency. The suppression of the peak is the result of an impurity limit imposed on the rapid increase in $\tau(T)$, which results in a limit on the initial rise in $\sigma_1(T)$ below T_c. The Zn impurities also give rise to a quadratic temperature dependence in $\sigma_1(T)$ at low temperatures. (b) shows that 0.75% Ni substitution (3.88 GHz, open triangles; 34.8 GHz, solid triangles) also suppresses the peak, but does not generate quadratic behavior at low temperatures.

or $\sigma_1(T)$. Nickel and zinc have qualitatively different effects on the low-temperature behavior of both $\Delta\lambda(T)$ and $\sigma_1(\omega,T)$.

V. MODELS OF THE SURFACE IMPEDANCE

There are two key conclusions that can be drawn from the foregoing surface-impedance measurements, independent of any models or microscopic theory. The first is that the impurity studies have rather solidly confirmed that a rapid increase in the quasiparticle lifetime below T_c is responsible for the large peak in $\sigma_1(T)$ in $YBa_3Cu_3O_{6.95}$. The dependence of the amplitude of the peak on frequency and impurity content points to an increase in $\tau(T)$ by roughly two orders of magnitude between T_c and 40 K. This conclusion can be made more quantitative by applying the generalized two-fluid model to extract $1/\tau(T)$ from the measurements of $R_s(T)$ and $\Delta\lambda(T)$. Equations (7)–(9), which are used to extract $\sigma_1(\omega,T)$ from $R_s(T)$ and $\Delta\lambda(T)$, are simply based on the electrodynamics of a local superconductor and the only significant assumption involved in extracting $\sigma_1(\omega,T)$ from our measurements is that a value for $\lambda(0)$ must be assumed in order to generate $\lambda(T)$ from $\Delta\lambda(T)$. Equation (11) defines the generalized two-fluid model that we use to try to interpret the data further. A division of oscillator strength between a normal-fluid term with weight $x_n(T)$ and a superfluid term with weight $x_s(T)$, where $x_s(t)=\lambda^2(0)/\lambda^2(T)$, is based on the sum rule that governs $\sigma_1(\omega)$ and the fact that it is the density of carriers in the superfluid term that is responsible for London screening at low frequencies. The weakest assumption of the model is the Drude form with a frequency-independent lifetime that we choose for the normal-fluid spectrum. This is likely an oversimplification, but in $YBa_2Cu_3O_{6.95}$ the temperature dependence of the scattering time is such a large effect that a Drude spectral shape is sufficient for modeling the main effects observed at microwave frequencies.

Figure 10 shows the scattering rate extracted from the measurements on the twin-free crystal. The small residual loss at low temperatures (5 $\mu\Omega$ at 4.13 GHz and 100 $\mu\Omega$ at 34.8 GHz) has been subtracted from the data sets before the analysis. The subtraction only has a significant effect on the inferred values of $1/\tau(T)$ below 10 K. Thus, insofar as the two-fluid analysis is valid, the values of $1/\tau(T)$ shown in Fig. 10 are reliable down to about 10 K. The two-fluid analysis of the 4.13-GHz data indicates that $1/\tau(T)$ falls by more than a factor of 100 from its value of 2.5×10^{13} s^{-1} just above T_c to a value of about 1.4×10^{11} s^{-1} at low temperatures. This implies that at low temperatures $\omega\tau=1.5$ at 34.8 GHz and places the low-temperature 34.8 GHz data in the regime where relaxation effects are important. The fact that $\omega\tau$ is of order unity is consistent with the observation that the σ_1(34.8 GHz, T) $\sim\frac{1}{2}\sigma_1$(4.13 GHz, T) below 30 K.

The quantitative differences between $1/\tau(T)$ inferred

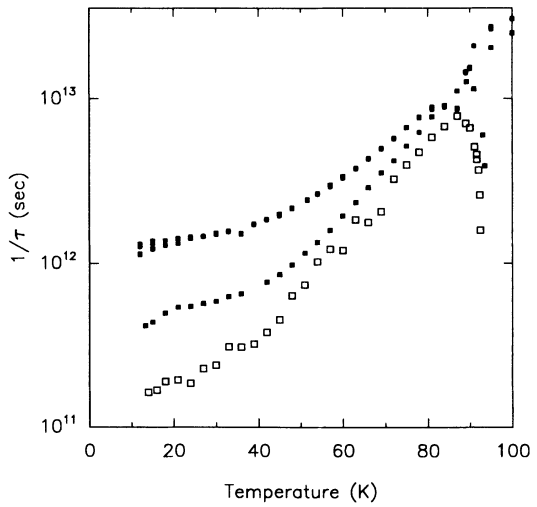

FIG. 10. The quasiparticle scattering rate inferred from the measurements of $\sigma_1(T)$ and $\Delta\lambda(T)$ for the twin-free crystal at 4.13 GHz (open squares) and 34.8 GHz (solid squares) shows a rapid decrease by a factor of 100 below T_c as the holes condense in the superconducting state. The differences between these two curves are due to inadequacies in the Drude line shape used to model the frequency dependence of the conductivity in the two-fluid model. The two-fluid analysis also indicates that the addition of 0.31% Zn impurities (solid circles) increases the limit that $1/\tau(T)$ runs into. This impurity limit on $1/\tau$ is the source of the suppression of $R_s(T)$ in impure samples.

from the data at the two different frequencies indicate that the Drude spectral shape does not adequately model all of the details of the conductivity. In the temperature range above 50 K, $\omega\tau \ll 1$ at both frequencies, and a Drude $\sigma_1(T)$ would be frequency independent. Instead, we find that $\sigma_1(T)$ is 30% larger at 4.13 GHz that it is at 34.8 GHz. This disagreement with the two-fluid model can be traced right back to the surface resistance where we find at high temperatures $R_s \propto \omega^{1.8}$ rather than the ω^2 behavior expected from the two-fluid model at low frequencies. This weaker frequency dependence is close to that observed in conventional superconductors where the diverging density of states at the gap edge leads to a logarithmic divergence in the frequency dependence of σ_1 at low frequency rather than the constant σ_1 of the two-fluid model. However, we have noted that the depth of the minimum in $R_s(T)$ is somewhat sample dependent and a small departure from ω^2 behavior in this temperature range may not be an intrinsic effect. At lower temperatures, where relaxation effects become important, the discrepancy in the $1/\tau$ inferred from the measurements at 4.13 and 34.8 GHz becomes quite large. This might be an indication of a frequency-dependent scattering rate, or it may also be a density of states effect. In an s-wave BCS superconductor, the effect of the diverging density of states gives conductivities near $\omega\tau \sim 1$ that differ substantially from those given by the Drude line shape.[48] So density of states effects, which require a more sophisticated model, might ultimately explain the finer details of $\sigma_1(\omega, T)$. Despite these limitations, the two-fluid model has appealing features. It provides a straightforward explanation of the peak in $\sigma_1(T)$ in terms of competition between $x_n(T)$ and $\tau(T)$, and it crudely accounts for the relaxation effects observed in the higher-frequency measurements.

The results from applying the two-fluid model to the 34.8-GHz measurements of the 0.31% Zn-doped sample are also included in Fig. 10. With the added impurity scattering, relaxation effects are not a problem and so the $1/\tau(T)$ at 34.8 GHz gives a reasonable measure of the effect of Zn on the scattering rate. The main result of the addition of the Zn impurities is an increase in the low-temperature limit of the scattering rate. At 0.31% doping, $1/\tau(T)$ runs into an impurity limit of 1.4×10^{12} s^{-1}. This impurity scattering can be compared to the results of Chien, Wang, and Ong[44] who have studied the dc transport properties of Zn-doped crystals above T_c. Using a ratio of the carrier density to effective mass, n/m^*, which is set by our choice of $\lambda(0)$, the increase in dc resistivity that Chien, Wang, and Ong observe corresponds to an increase in the scattering rate of 8×10^{12} per at. % substitution of Zn. So the dc resistivity measurements indicate an increase in the scattering rate of 2.5×10^{12} s^{-1} for a 0.31% Zn substitution, in reasonable agreement with the value that we infer from the microwave measurements below T_c. A two-fluid analysis of the conductivity of the 0.75% Ni-doped sample is rather uncertain because the residual loss is such a large fraction of the temperature-dependent loss. Nevertheless, the nearly complete suppression of the peak in the conductivity indicates that the Ni doping provides at least as much additional scattering as the Zn impurities.

The second solid conclusion that can be drawn from the surface-impedance measurements is that there is a spectrum of excitations in the superconducting state that extends to very low energies in $YBa_2Cu_3O_{6.95}$. In particular, the lack of exponentially activated behavior in either $R_s(T)$ or $\Delta\lambda(T)$ argues strongly against an s-wave BCS pairing state with a well-developed gap in the excitation spectrum. A number of studies of possible pairing mechanisms in high-T_c superconductors have pointed toward the possibility of a pairing state with d-wave symmetry.[49–51] Annett, Goldenfeld, and Renn have shown that such a pairing state in the crystal symmetry appropriate for $YBa_3Cu_3O_{6.95}$ would have line nodes in the gap function that lead to a linear temperature dependence in $\Delta\lambda(T)$ at low temperatures.[12] Given that a linear $\Delta\lambda(T)$ is in fact what we observe in our high quality crystals of $YBa_2Cu_3O_{6.95}$, the rest of the surface-impedance measurements should be examined in the light of this possibility. There is already a significant body of calculations of electromagnetic properties of anisotropic pairing states; earlier work aimed primarily at the heavy fermion superconductors,[4,21,52] and a more recent resurgence of interest in the context of high-temperature superconductors.[12,22,53] These studies include calculations of $\lambda(T)$, $\sigma_1(\omega, T)$, and the effects of impurities on superconductors with non-s-wave pairing states. In particular, recent calculations by Hirschfeld *et al.*[53] indicate that the linear behavior of $\Delta\lambda(T)$ should be accompanied by a quadratic temperature dependence for $\sigma_1(T)$ at low frequency ($\omega\tau \ll 1$). That is, for our nominally pure, twin-free sample the region below 25 K that exhibits the linear $\Delta\lambda(T)$ should be accompanied by quadratic behavior for $\sigma_1(T)$. Instead, we observe linear temperature dependence for $\sigma_1(T)$ at both 4.13 and 34.8 GHz in addition to the linear $\Delta\lambda(T)$. This asymptotic behavior of $\sigma_1(T)$ and $\Delta\lambda(T)$, shown in Fig. 11, is what one expects for a two-fluid model with a temperature-independent τ at low temperatures. Although the calculations of $\sigma_1(\omega, T)$ for a d-

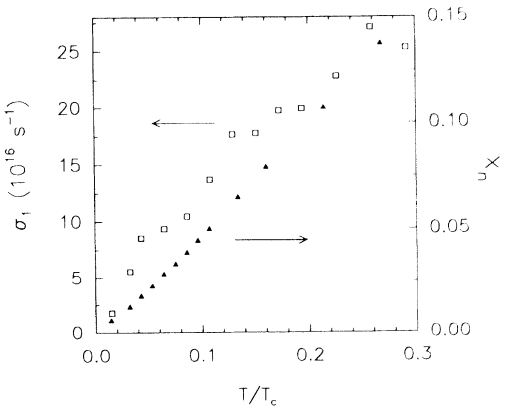

FIG. 11. Asymptotic behavior of the conductivity at 4.13 GHz (open squares) and the normal-fluid density (triangle). The linear behavior of $x_n(T)$ is consistent with a pairing state that has line nodes in the energy gap, but the linear behavior of $\sigma_1(T)$ is at odds with the T^2 temperature dependence expected for the conductivity of a d-wave superconductor.

wave superconductor can be cast in the form of a two-fluid model, they contain a frequency and temperature-dependent τ, even for impurity scattering. In particular, at low frequency and temperature, impurity scattering gives $\tau(T) \propto T$, which gives the extra power of T difference between $\Delta\lambda(T)$ and $\sigma_1(T)$ in the d-wave calculations.

The doped samples provide further tests of the interpretation of the low-temperature asymptotic behaviors. It has been well known that impurities, even nonmagnetic ones, can make a superconductor with a non-s-wave pairing state gapless and that a distinctive feature of this gapless state is quadratic behavior of $\Delta\lambda(T)$ at low temperatures.[21] Hirschfeld and Goldenfeld have shown that a small concentration of impurities in a d-wave superconductor can lead to a crossover from T^2 behavior at low temperatures to linear temperature dependence above some temperature T^*.[22] Furthermore, for resonant scattering the quadratic low-temperature regime should be in a measurable range for relatively small impurity concentrations that only have a small effect on T_c. The most obvious case for a crossover temperature is in the nominally pure samples which tend to show some curvature away from the linear temperature dependence below roughly 5 K. Similarly, Lee, Paget, and Lemberger have reported crossover behavior in thin films of $YBa_2Cu_3O_{7-\delta}$, though with a substantially higher crossover temperature of 25 K, presumably due to the higher level of defects in the thin films.[54] Figure 12 displays the behavior of the normal-fluid density, $x_n(T)=1-\lambda^2(0)/\lambda^2(T)$, for the pure and Zn-doped samples, along with fits to an interpolation formula $x_n(T)=aT^2/(T+T^*)$. These fits indicate that the crossover temperatures for the pure 0.15% Zn and 0.31% Zn samples are 3, 10, and 28 K, respectively. This sequence from the nominally pure sample with a low crossover temperature and predominantly linear temperature dependence to a Zn-doped sample with a high crossover temperature and predominantly quadratic behavior is in qualitative agreement with the theory of Hirschfeld and Goldenfeld.[22] Furthermore, the crossover temperatures are roughly those expected for resonant scatterers in a d-wave superconductor. For resonant scattering, $T^* \sim 0.83(\Gamma\Delta_0)^{1/2}$. The two-fluid analysis of the conductivity of the 0.31% Zn-doped sample indicated an impurity scattering rate of $\Gamma=1/(2\tau)\sim 5$ K. For an energy gap of $\Delta_0=3T_c$, this scattering rate gives $T^*=31$ K, quite close to the value inferred from the penetration-depth measurements. This T^* is high enough to almost completely eliminate the linear term in the penetration depth, leaving the quadratic behavior associated with a gapless superconductor. The low-temperature limit of the conductivity is also expected to be quadratic in the gapless regime, as is observed for the 0.31% Zn-doped sample at 34.8 GHz. Figure 13 focuses in on the quadratic behavior of both $x_n(T)$ and $\sigma_1(34.8\ \text{GHz},T)$ for the 0.31% Zn-doped sample at low temperatures.

Ni impurities do not fit into the same scheme of resonant scattering that seems to give a reasonable description of the Zn impurity effects. The 0.75% Ni impurity level suppresses T_c nearly as much as the 0.31% Zn and provides at least as much scattering as the Zn impurities, but does not produce any quadratic, gapless behavior in either $\Delta\lambda(T)$ or $\sigma_1(T)$. It is tempting to suggest that Ni might be a nonresonant scatterer and that results for the Born limit rather than the unitary limit are more appropriate. The T^* for a Born scatterer is given approximately by $\Delta_0 e^{-\Delta_0/\Gamma}$, which gives a much lower crossover temperature for a given scattering rate Γ than does the resonant scattering result. This could explain the per-

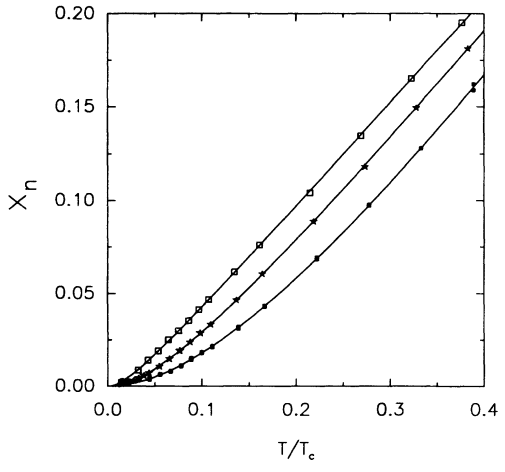

FIG. 12. Low-temperature behavior of the normal-fluid density $x_n(T)=1-\lambda^2(0)/\lambda^2(T)$ in the nominally pure crystal (open squares) and the samples doped with 0.15% (stars) and 0.31% (solid circles) Zn. The solid lines are fits to an interpolation formula $x_n(T)=aT^2/(T+T^*)$, which models the crossover from quadratic behavior at low temperatures to linear behavior at higher temperatures. For the pure crystal the crossover temperature is low, $T^* \sim 3$ K, but with the addition of 0.31% Zn, $T^* \sim 30$ K and the linear regime is almost completely eliminated.

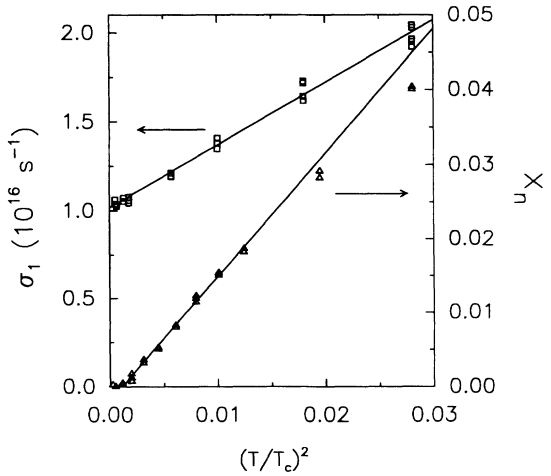

FIG. 13. Asymptotic behavior of the normal-fluid density (triangles) and 34.8-GHz conductivity (squares) vs. the square of the reduced temperature for the 0.31% Zn-doped sample. The quadratic temperature dependence of both quantities indicates that this low level of Zn impurities leads to gapless superconductivity in $YBa_2Cu_3O_{6.95}$.

sistence of the linear $\Delta\lambda(T)$ in the Ni-doped sample, but such a huge difference in the nature of the scattering for the two impurities bears closer examination.

VI. CONCLUSIONS

The striking qualitative features of the surface impedance of high purity crystals of $YBa_2Cu_3O_{6.95}$ lead to two far-reaching conclusions about the fundamental properties of this high-T_c superconductor. The broad peak in the surface resistance indicates that the quasiparticle scattering rate drops dramatically below T_c, falling from the large value caused by inelastic scattering above T_c to a low value that is controlled by impurity scattering in the superconducting state. This phenomenon has manifested itself in far-infrared,[36] THz spectroscopy,[34] and thermal conductivity[37] measurements as well as the surface resistance and must be taken into account in the interpretation of any property in the superconducting state that is sensitive to the quasiparticle scattering rate. The fact that the inelastic scattering collapses as the holes condense in the superconducting state makes it clear that the large scattering rate in the normal state is primarily *electronic* in origin; there is neither a significant impurity nor a large phonon contribution to the scattering rate above T_c.

The linear temperature dependence observed for $\Delta\lambda(T)$ and $\sigma_1(T)$ at low temperatures indicates that there is a spectrum of excitations down to very low energies in the superconducting state. This linear behavior is quite unlike the exponentially activated behavior caused by the nodeless energy gap of a conventional *s*-wave BCS superconductor. Instead, the linear temperature dependence of $\Delta\lambda(T)$ is the asymptotic behavior expected for a *d*-wave pairing state with line nodes in the energy gap. However, present calculations indicate that a *d*-wave pairing state with line nodes should have quadratic temperature dependence for $\sigma_1(T)$, rather than the linear behavior that we observe for $YBa_2Cu_3O_{6.95}$. It is not yet clear whether this discrepancy is evidence against a *d*-wave pairing state or is the result of some assumption built into the theoretical calculations of $\sigma_1(\omega,T)$.

The fact that it has taken years to uncover these clear, qualitative features of the surface impedance of pure $YBa_2Cu_3O_{6.95}$ is a testament to the sensitivity of these properties to the presence of defects. This sensitivity has two sources. Most obviously, impurities control the size of the drop in the quasiparticle scattering rate below T_c and the effect that this has on the microwave surface resistance is clearly demonstrated by the decrease in $R_s(T)$ with the addition of either Zn or Ni impurities. The second, more subtle, effect that impurities can have is to push $YBa_2Cu_3O_{6.95}$ into a gapless state. Addition of as little as 0.15 % Zn impurities alters the linear behavior of $\Delta\lambda(T)$ and 0.31% Zn makes both $\Delta\lambda(T)$ and $\sigma_1(T)$ quadratic, clear signs of gapless superconductivity. Further evidence for gapless superconductivity in Zn-doped $YBa_2Cu_3O_{7-\delta}$ includes a linear term in the electronic specific heat at low temperature that increases in magnitude as Zn is added[55] and NMR measurements that show Korringa behavior at low T for $1/T_1T$ when 1–2 % Zn impurities are introduced.[56] Although there is some controversy regarding the effect that Zn impurities have on the magnetic susceptibility,[57,58] the NMR results seem to indicate that the Zn ions are entering the lattice as a nonmagnetic impurity.[56] If this is indeed the case, the fact that we observe gapless behavior for as little as 0.31% substitution of a nonmagnetic impurity is in itself evidence for a pairing state other than the usual *s*-wave BCS pairing.

There is a further connection between the impurity studies presented here and the NMR results. Although the NMR measurements indicate that there is a local moment associated with Ni impurities, there is no sign of gapless behavior in the NMR measurements of a sample containing 1% Ni impurities.[56] Despite the fact that the Zn impurities are nonmagnetic and the Ni impurities are magnetic, both the microwave and NMR measurements indicate that small levels of Zn impurities make $YBa_2Cu_3O_{7-\delta}$ gapless, but Ni impurities do not. This result is the opposite of that expected in an *s*-wave superconductor. Although the difference between these impurities might be attributed to a difference in their scattering strength, Zn being a resonant scatterer and Ni a Born scatterer, the NMR measurements suggest a situation that is rather complicated in detail. A key difference between Ni and Zn is that the Zn impurities alter the local spin fluctuations in the CuO_2 planes,[56] a difference that has been suggested as an explanation for the stronger influence that Zn impurities have on T_c.[59] Taken altogether, the NMR and microwave measurements indicate a material with strong antiferromagnetic spin fluctuations and large inelastic scattering of charge carriers in the normal state and on unconventional pairing state consistent with line nodes in the energy gap in the superconducting state. The striking difference between the effects of Ni and Zn impurities on all of these properties provides a rich basis for testing microscopic theories of both the normal state and superconductivity in $YBa_2Cu_3O_{7-\delta}$.

ACKNOWLEDGMENTS

We have benefited from many helpful discussions with T. Timusk, P. Stamp, D. J. Scalapino, P. Hirschfeld, N. Goldenfeld, C. Kallin, A. J. Berlinsky, J. P. Carbotte, E. Nicol, P. Monthoux, and D. Pines. We are also indebted to Pinder Dosanjh and the staff of the UBC machine shop for technical assistance. This work was supported by grants from the Natural Sciences and Engineering Research Council of Canada and by the Canadian Institute for Advanced Research.

*Permanent address: Dept. of Physics, Freie Universität Berlin, Arnimallee 14, 1000 Berlin 33, Germany.

[1]Tetsuya Hasegawa, Hiroshi Ikuta, and Koichi Kitazawa, in *Physical Properties of High-Temperature Superconductors,* edited by Donald M. Ginsberg (World Scientific, Singapore, 1992), Vol. 3.

[2]K. Kamarás, S. L. Herr, C. D. Porter, N. Tache, D. B. Tanner, S. Etemad, T. Venkatesan, E. Chase, A. Inam X. D. Wu, M.

S. Hegde, and B. Dutta, Phys. Rev. Lett. **64**, 84 (1990).
[3]M. Reedyk and T. Timusk, Phys. Rev. Lett. **69**, 2705 (1992).
[4]R. A. Klemm, K. Scharnberg, D Walker, and C. T. Rieck, Z. Phys. B **72**, 139 (1988).
[5]D. R. Harshman, L. F. Schneemeyer, J. V. Waszczak, G. Aeppli, R. J. Cava, B. Batlogg, L. W. Rupp, E. J. Ansaldo, and D. Ll. Williams, Phys. Rev. B **39**, 851 (1989).
[6]B. Pümpin, H. Keller, W. Kündig, W. Odermatt, I. M. Savic, J. W. Schneider, H. Simmler, P. Zimmermann, J. G. Bednorz, Y. Maeno, K. A. Müller, C. Rossel, E. Kaldis, S. Rusiecki, W. Assmus, and J. Kowalewski, Physica C **151-152**, 151 (1989).
[7]J. E. Sonier, R. F. Kiefl, J. H. Brewer, D. A. Bonn, J. F. Carolan, K. H. Chow, P. Dosanjh, W. N. Hardy, Ruixing Liang, W. A. MacFarlane, P. Mendels, G. D. Morris, T. M. Riseman, and J. W. Schneider, Phys. Rev. Lett. **72**, 744 (1994).
[8]D. A. Bonn, Ruixing Liang, T. M. Riseman, D. J. Baar, D. C. Morgan, Kuan Zhang, P. Dosanjh, T. L. Duty, A. MacFarlane, G. D. Morris, J. H. Brewer, W. N. Hardy, C. Kallin, and A. J. Berlinsky, Phys. Rev. B **47**, 11 314 (1993).
[9]A. Porch, J. R. Cooper, D. N. Zheng, J. R. Waldram, A. M. Campbell, and P. A. Freeman, Physica C **214**, 350 (1993).
[10]A. M. Neminsky and P. N. Nikolaev, Physica C **212**, 389 (1993).
[11]A. T. Fiory, A. F. Hebard, P. M. Mankiewich, and R. E. Howard, Phys. Rev. Lett. **61**, 1419 (1988).
[12]J. A. Annett, N.Goldenfeld, and S. R. Renn, Phys. Rev. B **39**, 2778 (1991).
[13]L. Kruisin-Elbaum, R. L. Greene, F. Holtzberg, A. P. Malozemoff, and Y. Yeshurun, Phys. Rev. Lett. **62**, 217 (1989).
[14]Hong Ning, H. Duan, P. D. Kirven, A. M. Hermann, and T. Datta, J. Supercond. **5**, 903 (1993).
[15]W. N. Hardy, D. A. Bonn, D. C. Morgan, Ruixing Liang, and Kuan Zhang, Phys. Rev. Lett. **70**, 3999 (1993).
[16]J. M. Pond, K. R. Carroll, J. S. Horowitz, D. B. Chrisey, M. S. Osofsky, and V. C. Cestone, Appl. Phys. Lett. **59**, 3033 (1991).
[17]S. M. Anlage and Dong-Ho Wu, J. Supercond. **5**, 395 (1992).
[18]Zhen Xiang Ma, R. C. Taber, L. W. Lombardo, A. Kapitulnuk, M. R. Beasley, P. Merchant, C. B. Eom, S. Y. Hou, and Julia M. Phillips, Phys. Rev. Lett. **71**, 781 (1993).
[19]J. Y. Lee and T. Lemberger, Appl. Phys. Let. **62**, 2419 (1993).
[20]Steven M. Anlage, Brian W. Langley, Guy Deutscher, Jürgen Halbritter, and M. R. Beasley, Phys. Rev. B **44**, 9764 (1991).
[21]F. Gross, B. S. Chandrasekhar, D. Einzel, K. Andres, P. J. Hirschfeld, H. R. Ott, J. Beuers, Z. Fisk, and J. L. Smith, Z. Phys. B **64**, 175 (1986).
[22]Peter J. Hirschfeld and Nigel Goldenfeld, Phys. Rev. B **48**, 4219 (1993).
[23]M. Lippert, J. P. Ströbel, G. Saemann-Ischenko, S. Orbach, S. Hensen, G. Müller, H. Piel, J. Schützmann, K. F. Renk, B. Roas, and W. Gieres, Physica C **185-189**, 1041 (1991).
[24]Kuan Zhang, D. A. Bonn, Ruixing Liang, D. J. Baar, and W. N. Hardy, Appl. Phys. Lett. **62**, 3019 (1993).
[25]D. A. Bonn, Kuan Zhang, Ruixing Liang, D. J. Baar, D. C. Morgan, and W. N. Hardy, J. Supercond. **6**, 219 (1993).
[26]D. A. Bonn, D. C. Morgan, Kuan Zhang, Ruixing Liang, D. J. Baar, and W. N. Hardy, J. Phys. Chem. Solids **54**, 1297 (1993).
[27]D. A. Bonn, P. Dosanjh, R. Liang, and W. N. Hardy, Phys. Rev. Lett. **68**, 2390 (1992).
[28]T. Shibauchi, A. Maeda, H. Kitano, T. Honda, and K. Uchinokura, Physica C **203**, 315 (1992).
[29]N. Klein, U. Dähne, U. Poppe, N. Tellmann, K. Urban, S. Orbach, S. Hensen, G. Müller, and H. Piel, J. Supercond. **5**, 195 (1992).
[30]D. A. Bonn, D. C. Morgan, and W. N. Hardy, Rev. Sci. Instrum. **62**, 1819 (1991).
[31]Ruixing Liang, P. Dosanjh, D. A. Bonn, D. J. Baar, J. F. Carolan, and W. N. Hardy, Physica C **195**, 51 (1992).
[32]D. Achkir, M. Poirier, D. A. Bonn, Ruixing Liang, and W. N. Hardy, Phys. Rev. B **48**, 13 184 (1993).
[33]D. M. Basov, A. V. Puchkov, R. A. Hughes, T. Strach, T. Timusk, D. A. Bonn, R. Liang, and W. N. Hardy (unpublished).
[34]Martin C. Nuss, P. M. Mankiewich, M. L. O'Malley, E. H.Westerwick, and Peter B. Littlewood, Phys. Rev. Lett. **66**, 3305 (1991).
[35]P. B. Littlewood and C. M. Varma, Phys. Rev. B **46**, 405 (1992).
[36]D. B. Romero, C. D. Porter, D. B. Tanner, L. Forro, D. Mandrus, L. Mihaly, G. L. Carr, and G. P. Williams, Phys. Rev. Lett. **68**, 1590 (1992).
[37]R. C. Yu, M. B. Salamon, J. P. Lu, and W. C. Lee, Phys. Rev. Lett. **69**, 1431 (1992).
[38]J. L. Cohn, V. Z. Kresin, M. E. Reeves, and S. A. Wolf, Phys. Rev. Lett. **71**, 1657 (1993).
[39]R. C. Yu, M. B. Salamon, and J. P. Lu, Phys. Rev. Lett. **71**, 1658 (1993).
[40]M. J. Rice and Y. R. Wang, Bull. Am. Phys. Soc. **34**, 517 (1989); (unpublished).
[41]D. B. Tanner and T. Timusk, in *Physical Properties of High-Temperature Superconductors,* edited by Donald M. Ginsberg (World Scientific, Singapore, 1992), Vol. 3.
[42]H. Maeda, A. Koizumi, N. Bamba, E. Takayama-Muromachi, F. Izumi, H. Asano, K. Shimizu, H. Moriwaki, H. Maruyama, Y. Kuroda, and H. Yamazaki, Physica C **157**, 483 (1989).
[43]Frank Bridges, Guoguang Li, James B. Boyce, Tord Claeson, and H. Wühl (unpublished).
[44]T. R. Chien, Z. Z. Wang, and N. P. Ong, Phys. Rev. Lett. **67**, 2088 (1991).
[45]Michael J. Sumner, Jin-Tae Kim, and Thomas R. Lemberger, Phys. Rev. B **47**, 12 248 (1993).
[46]F. Marsiglio, Phys. Rev. D **44**, 5373 (1991).
[47]R. Akis and J. P. Carbotte, Solid State Commun. **79**, 577 (1991).
[48]A. J. Berlinsky, C. Kallin, G. Rose, and A.-C. Shi, Phys. Rev. B **48**, 4074 (1993).
[49]P. A. Lee and N. Read, Phys. Rev. Lett. **58**, 2691 (1987).
[50]C. Gros, R. Joynt, and T. M. Rice, Z. Phys. B **68**, 425 (1987).
[51]P. Monthoux, A. V. Balatsky, and D. Pines, Phys. Rev. Lett. **67**, 3448 (1991).
[52]P. J. Hirschfeld, P. Wölfe, J. A. Sauls, D. Einzel, and W. O. Putikka, Phys. Rev. B **40**, 6695 (1989).
[53]P. J. Hirschfeld, W. O. Putikka, and D. J. Scalapino, Phys. Rev. Lett. **71**, 3705 (1993).
[54]Ju Young Lee, Kathleen Paget, and Thomas R. Lemberger (unpublished).
[55]J. W. Loram, K. A. Mitza, and P. F. Freeman, Physica C **171**, 243 (1990).
[56]K. Ishida, Y. Kitaoka, N. Ogata, T. Kamino, K. Asayama, J. R. Cooper, and N. Athanassopoulou, J. Phys. Soc. Jpn. **62**, 2803 (1993).
[57]H. Alloul, P. Mendels, H. Casalta, J. F. Marucco, and J. Arabski, Phys. Rev. Lett. **67**, 3140 (1991).
[58]J. R. Cooper, Supercond. Sci. Technol. **4**, 181 (1991).
[59]P. Monthoux and D. Pines, Phys. Rev. B **49**, 4261 (1994).